

Biaxial creep property of ethylene tetrafluoroethylene (ETFE) foil

Yintang Li and Minger Wu*

Department of Structural Engineering, Tongji University, Shanghai, China

(Received July 23, 2014, Revised December 23, 2014, Accepted April 16, 2015)

Abstract. Ethylene tetrafluoroethylene (ETFE) foil is a novel structural material which has been used in shell and spatial structures. This paper studies biaxial creep property of ETFE foil by creep tests and numerical simulation. Biaxial creep tests of cruciform specimens were performed using three stress ratios, 1:1, 2:1 and 1:2, which showed that creep coefficients in biaxial tension were much smaller than those in uniaxial one. Then, a reduction factor was introduced to take account of this biaxial effect, and relation between the reduction factor and stress ratio was established. Circular bubble creep test and triangle cushion creep test of ETFE foil were performed to verify the relation. Interpolation was adopted to consider creep stress and reduction factor was involved to take account of biaxial effect in numerical simulation. Simulation results of the bubble creep test embraced a good agreement with those measuring ones. In triangle cushion creep test, creep displacements from numerical simulation showed a good agreement with those from creep test at the center and lower foil measuring points.

Keywords: ETFE foil; cushion; biaxial creep; creep test; creep simulation

1. Introduction

Recent decades have witnessed a great success of ethylene tetrafluoroethylene (ETFE) foil being used as roofs and claddings in long-span buildings, with some impressive constructions like the Allianz Arena in Germany (2006) and the National Aquatics Center in China (2008) (Robinson-Gayle *et al.* 2001, LeCuyer 2008). For the extremely thin property, usually 50 μm to 300 μm in thickness, ETFE foil is treated as membrane and could only be tensioned in structures. The most common structural type of ETFE foil is double-layer or multi-layer cushion, which is supported by inner air pressure (Wu and Liu 2008). It has distinctive advantages in architecture facade, structural reliability and energy efficiency (Hu *et al.* 2014, Zhang *et al.* 2014).

As a novel structural material, ETFE foil has been studied by researchers through tests and numerical simulation, especially for its mechanical properties. De Focatiis and Gubler (2013) studied uniaxial tensile property of ETFE foil from different manufacturers, all showing two yield points and strain hardening characteristics. Hu and Chen (2014) analyzed cyclic elastic modulus of ETFE foil by eight kinds of uniaxial cyclic tensile experiments. To investigate mechanical

*Corresponding author, Professor, E-mail: wuminger@tongji.edu.cn

properties of ETFE foil between the first and the second yield points, Kawabata (2007) performed cyclic tension tests for elongation analysis. On the other hand, Galliot and Luchsinger (2011) compared uniaxial and biaxial mechanical properties of this material by tests and Finite Element Method (FEM). Three tests, namely uniaxial tensile test, biaxial tensile test and bubble test, all exhibited similar tensile properties before the second yield point.

ETFE foil exhibits viscoelastic and viscoplastic properties in its long serving life, which would lead to creep deformation in ETFE cushion. This creep deformation decreases the beauty of architecture and has a negative effect on the safety of structure. To consider the mechanics of such time-dependent materials, Schapery (1969) established nonlinear viscoelastic constitutive equations in single integral form, which has been applied to polyethylene (Papanicolaou *et al.* 1999a, b), hybrid composites (Kim and Muliana 2010) and laminated glass (Huang *et al.* 2014). Meanwhile, Williams, Landel and Ferry (1955) found a relation between relaxation time and temperature, namely time-temperature superposition, to predict long-term creep property of such materials. Additionally, Pandini and Pegoretti (2011) studied Poisson's ratio of polymer and its dependence on time, temperature and strain rate. When it turns to ETFE foil, Kawabata and Moriyama (2006) took series of uniaxial creep tests and developed traditional viscoelastic modelling to consider its plastic strain. Charbonneau *et al.* (2014) presented uniaxial tests of ETFE foil under different time scales and stresses, and proposed a standard modelling in the integral form.

To simulate creep behaviors of materials and structures, Kennedy and Wang (1994, 1998) presented finite element analysis for viscoelastic response of laminated composites. Wu and Li (2014) developed their work to consider viscoelastic-plastic behavior of time-dependent materials. Klosowski *et al.* (2009) proposed nonlinear viscoelastic description of textile materials, such as PVC. Furthermore, Chazal and Pitti (2011) presented an approach for the solution of linear, non-aging viscoelastic materials to discretize the integral operators. Chung and Ryou (2009a, b) developed viscoelastic/rate-sensitive-plastic constitutive law for fiber reinforced composites and applied it in both loading process and creep analysis.

However, while prior researches mostly study viscoelastic or viscoelastic-plastic property of polymers on the basis of uniaxial creep tests, ETFE foil is always biaxial tensioned in cushion. That is to say, when ETFE foil is supported by inner pressure or bearing loads in its serving life, this material creeps in biaxial tension condition, rather than uniaxial one. Until now, less work has been done on biaxial creep test or biaxial creep property of ETFE foil.

In present work, biaxial creep property of ETFE foil is investigated. (1) Biaxial creep tests of cruciform samples were done using three stress ratios, which showing the difference between uniaxial and biaxial creep properties. (2) To unify uniaxial creep coefficients and biaxial ones, a reduction factor is introduced. The reduction factor is written as a function of stress ratio. Biaxial creep strain could then be determined by this reduction factor and uniaxial creep coefficients. (3) Bubble creep test and triangle cushion creep test were also performed to verify the relation of reduction factor and stress ratio. Biaxial creep coefficients of ETFE foil are determined and numerical simulations are done.

2. Material and methods

2.1 Material

ETFE foil used in this paper was produced by Asahi Glass Company. Density of this material is 1.7 g/cm³ and light transmission is about 95 %. All foils are 250 μm in thickness, which is commonly used in cushion structures.

Statistical uniaxial mechanical coefficients of ETFE foil are listed in Table 1. For the tiny deviation of mechanical properties in two directions, namely the machine direction (MD) and the transverse direction (TD), ETFE foil is regarded as isotropic material in this paper. These tensile coefficients were obtained from 10 specimens with tensile strain rate at 100 %/min.

2.2 Uniaxial creep coefficients

Basing on Schapary’s single integral form, a revised viscoelastic-plastic modelling is simplified to simulate creep behavior of ETFE foil, as shown in Eq. (1) and Eq. (2) (Li and Wu 2015).

$$\varepsilon(t)=(D_0 + D_{ve} + D_{vp})\sigma \tag{1}$$

$$D_{ve} = \sum_{r=1}^n D_r (1 - e^{-\frac{t}{10^r}}) \text{ and } D_{vp} = D_s t^k \tag{2}$$

where $\varepsilon(t)$ is the strain being dependent on time, σ is the stress, D_0 is initial compliance, D_{ve} is viscoelastic compliance, D_{vp} is viscoplastic compliance, D_r , D_s and k are creep coefficients in transient compliance, n is the number of the generalized Kelvin components.

The first term of Eq. (1) is initial compliance of ETFE foil. This term is represented by a spring in the rheological model as shown in the left side of Fig. 1. Its coefficient is the same as that in uniaxial test, as studied by Galliot and Luchsinger (2011). The second term of Eq. (1) is a part of transient compliance. It is simplified as generalized Kelvin model and illustrated in the middle of Fig. 1. To cover the range of creep time in all tests and get creep coefficients precisely, the number of generalized Kelvin components n is set as 5 and the retard time is 10⁵. The third term of Eq. (1) is the other part of transient compliance. It increases during creep time but would not recover even when the stress turned zero. So, it is represented by a dashpot in Fig. 1.

As shown in Eq. (2), viscoelastic component represents creep compliance that can recover in a given time, while viscoplastic component represents that unrecoverable one. To obtain creep coefficients in Eq. (2), assumes are made that creep behavior is a summation of viscoelastic and viscoplastic creep, and recovery behavior is the inverse process of viscoelastic creep, in which no viscoplastic creep occurs. All of these coefficients are obtained from creep and recovery tests. The

Table 1 Mechanical properties of ETFE foil in uniaxial test

Strain Rate	First Yield Point		Second Yield Point		Tensile at Failure	
	Stress	Strain	Stress	Strain	Stress	Strain
100 %/min	16.9MPa	2.7%	23.5MPa	15.3%	49.5MPa	440%

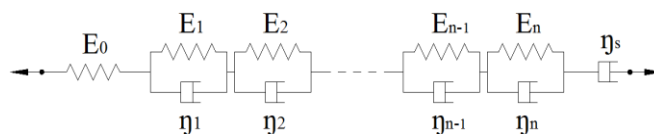


Fig. 1 Rheological model for the constitutive equation

Table 2 Creep coefficients of ETFE foil in uniaxial test

	σ	D_0	D_1	D_2	D_3	D_4	D_5	D_s	n
S-1	3 MPa	1.156E-3	6.085E-5	3.895E-5	5.742E-5	5.020E-5	4.986E-5	1.371E-6	0.36212
	6 MPa	1.171E-3	6.330E-5	4.767E-5	7.837E-5	8.295E-5	6.204E-5	1.383E-6	0.43448
	9 MPa	1.205E-3	1.146E-4	1.658E-4	3.600E-4	4.045E-4	3.238E-4	1.991E-6	0.60991
S-2	3 MPa	1.228E-3	2.770E-6	4.597E-6	3.145E-5	4.869E-5	4.757E-5	1.635E-7	0.53887
	6 MPa	1.296E-3	8.311E-6	5.617E-5	1.466E-4	1.937E-4	1.110E-4	9.752E-7	0.54189
	9 MPa	1.378E-3	1.334E-5	1.349E-4	3.667E-4	3.970E-4	2.419E-4	5.319E-7	0.69900
	12 MPa	1.431E-3	2.380E-5	2.303E-4	4.588E-4	3.711E-4	4.251E-4	1.554E-5	0.43873

process of these creep and recovery tests is listed below. At first, specimens were tensioned to creep stress by a stress rate (1.8 MPa/s in S-1 and 0.1 MPa/s in S-2). Then creep tests began and lasted for 24 hours. After 24 creep hours, stress decreased to zero by the identical stress rate (1.8 MPa/s in S-1 and 0.1 MPa/s in S-2). Finally, recovery tests started and lasted another 24 hours when the stress kept zero. Initial compliances are determined by loading and unloading process. Coefficients in viscoelastic part (D_1 to D_5) are fitted by the least squared method according to recovery curves and coefficients in viscoplastic part, namely D_s and n , are fitted on the basis of creep curves after D_r are determined. Creep coefficients in two series are listed in Table 2.

As listed in Table 2, two series (S-1 and S-2) of uniaxial creep and recovery tests were performed under different stresses. These stresses were set to cover the highest design stress of ETFE foil, normally no more than one fourth of its tensile fracture strength. Meanwhile, because creep coefficients in uniaxial and biaxial tests are compared in the following part, stresses in these two series were set to be consistent with those in three biaxial creep tests. Specifically, stresses in S-1 were identical to those in biaxial creep tests of cruciform specimens, and stresses in S-2 covered the stress range in bubble creep test and cushion creep test. For similar reason, ETFE foil in S-1 was cut from cruciform specimens and strain rate in S-1 was set similar to that in biaxial creep tests of cruciform specimens. Material in S-2 was obtained from specimens in bubble creep test and cushion creep test. Strain rate in S-2 was also similar to that in bubble and cushion creep tests.

For the control of temperature in all creep tests, with an average of 20°C, temperature effect is not discussed in this paper.

As shown in Table 2, uniaxial creep coefficients, namely D_0 , D_r , D_s and n , all have a relation with stress. Therefore, interpolation method is adopted to determine uniaxial creep coefficients according to different stresses. This method is described by Eq. (3). While D_0 , D_r and n are obtained from linear interpolation, D_s is obtained from interpolation by proportional parts, for the coupling of D_s and n in coefficients fitting.

$$\begin{aligned}
 D_0(\sigma) &= D_0(\sigma_i) + \frac{D_0(\sigma_j) - D_0(\sigma_i)}{\sigma_j - \sigma_i} (\sigma - \sigma_i) \\
 D_r(\sigma) &= D_r(\sigma_i) + \frac{D_r(\sigma_j) - D_r(\sigma_i)}{\sigma_j - \sigma_i} (\sigma - \sigma_i) \\
 n(\sigma) &= n(\sigma_i) + \frac{n(\sigma_j) - n(\sigma_i)}{\sigma_j - \sigma_i} (\sigma - \sigma_i) \\
 D_s(\sigma) &= D_s(\sigma_i)^{\frac{\sigma_j - \sigma}{\sigma_j - \sigma_i}} \times D_s(\sigma_j)^{\frac{\sigma - \sigma_i}{\sigma_j - \sigma_i}}
 \end{aligned} \tag{3}$$

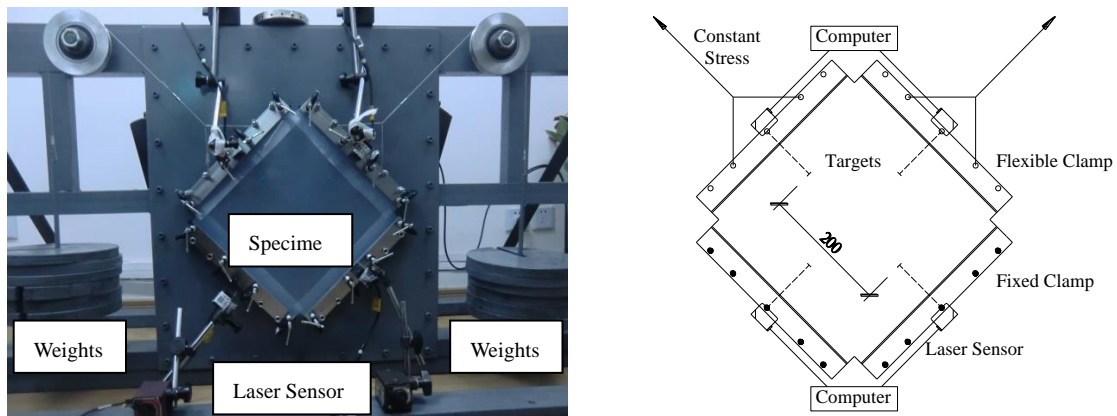


Fig. 2 Biaxial creep test and cruciform specimen

where σ_i and σ_j are the stresses in uniaxial creep tests and listed in Table 2, $\sigma_i \leq \sigma < \sigma_j$.

2.3 Biaxial creep tests of cruciform specimens

Cruciform shaped specimens are used for biaxial tensile tests of membranes, traditionally for coated fabrics PVC and PTFE (Ambroziak and Klosowski 2014), and recently for thermoplastic foil ETFE (Galliot and Luchsinger 2011). This kind of tests is practicable to investigate biaxial creep property of ETFE foil under identical stress.

To generate a constant stress in the tests, equipment for the biaxial creep tests of cruciform specimens was designed and illustrated in Fig. 2. This equipment offered constant stress by weights and oriented direction of stress by fixed pulleys. Non-contact laser sensors were used for creep displacement measurement. Measuring range of laser sensors used in these tests was 10.00 mm and the accuracy was $\pm 0.1\%$. Cruciform specimens designed for these tests were in square shape of 300.0 mm in length, with addition 15.0 mm arm in each edge. Because the accuracy of laser sensors was ± 0.01 mm, which calling for longer measuring distance (meaning longer creep displacement) to get more exact creep data, the recorded distance of creep displacement in each direction was set as the core 200.0 mm. In addition, to make the loading conditions in two sides be identical and enable the directions of two sides be symmetry, plate of specimens was set vertical to the ground and turned to 45 degrees in biaxial creep tests of cruciform specimens.

In biaxial creep tests of cruciform specimens, stress ratios of the machine direction (MD) to the transverse direction (TD) were 1:1, 2:1 and 1:2. The number of specimens for each stress ratio was two. Maximum stress was set as 6 MPa and minimum stress was 3 MPa. In the loading process, stresses were generated in third steps. Each step loaded one-third weights and the time between two steps was about 2 seconds, in which the time of loading process was similar to those in S-1 uniaxial creep tests. It enables similar strain rate in uniaxial and biaxial creep tests, because strain rate has significant effect on time dependent behavior of ETFE foil. Creep time of these tests was 24 hours and temperature during creep tests was $20 \pm 1^\circ\text{C}$.

2.4 Bubble creep test

Because creep displacement in biaxial creep tests of cruciform specimens was quite small,

bubble creep test was adopted in this section. This test is suitable to investigate creep displacement of ETFE foil in larger dimension and higher stress. Also, the air loading method is similar to that in ETFE cushion structures.

Equipment used in this test contained a steel plate and a steel ring, as shown in Fig. 3. Two holes were leaving for air inflation and pressure sensor in the steel plate. The range of pressure sensor was 2000 Pa and the accuracy was $\pm 0.5\%$. Pressure data was recorded as synchronous transport signal in the test. The plate and the ring were connected by 36 bolts and butyl tapes to avoid air leakage. Additionally, measuring range of laser sensors for creep test was 40.00 mm and their accuracy was $\pm 0.15\%$. Radius of circular specimen was 500.0 mm. Six displacement measuring points (C1 - C6) were set in the specimen. Detailed locations of these measuring points were illustrated in Fig. 4.

In the test, flat circular specimen of ETFE foil was clamped between the plate and the ring. To control similar strain rate in uniaxial and biaxial creep tests as stated in section 2.3, air was gassed

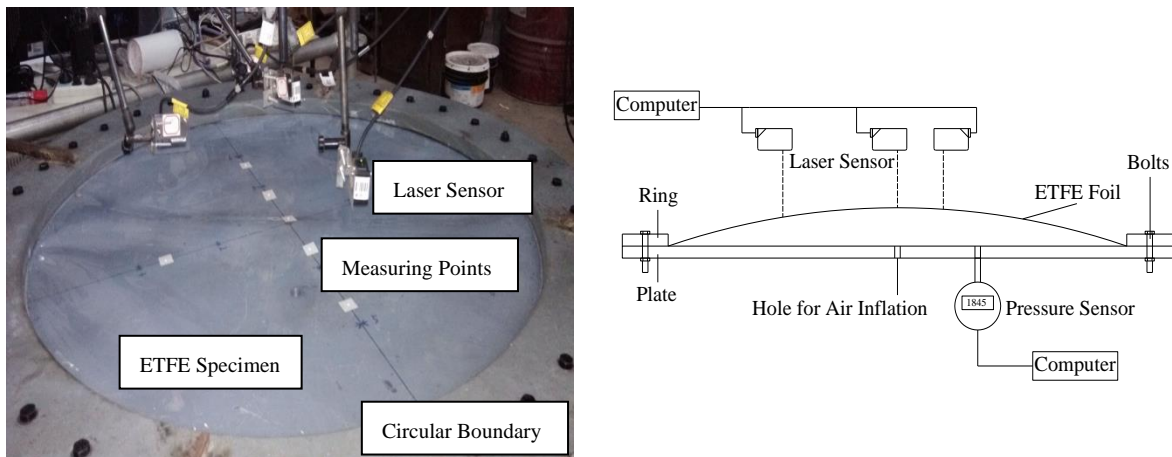


Fig. 3 Bubble creep test

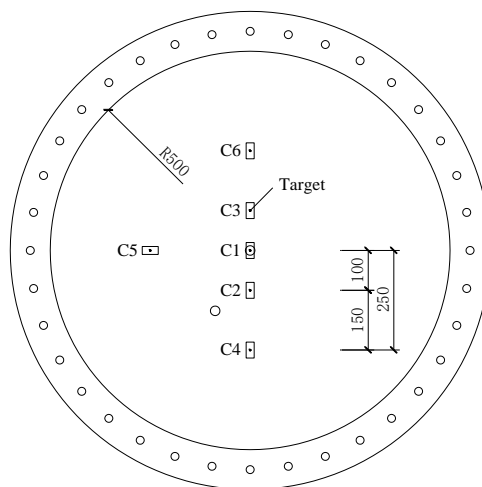


Fig. 4 Creep displacement measuring points in bubble creep test

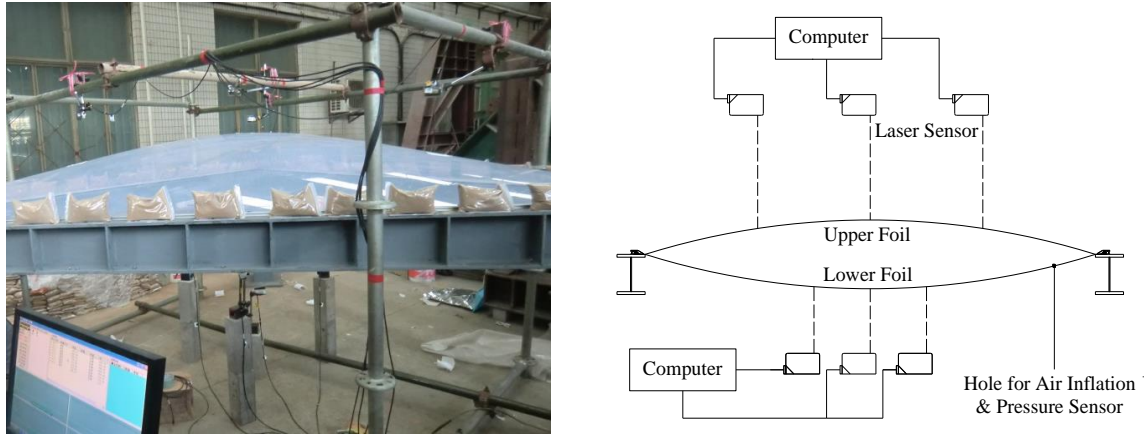


Fig. 5 Cushion creep test

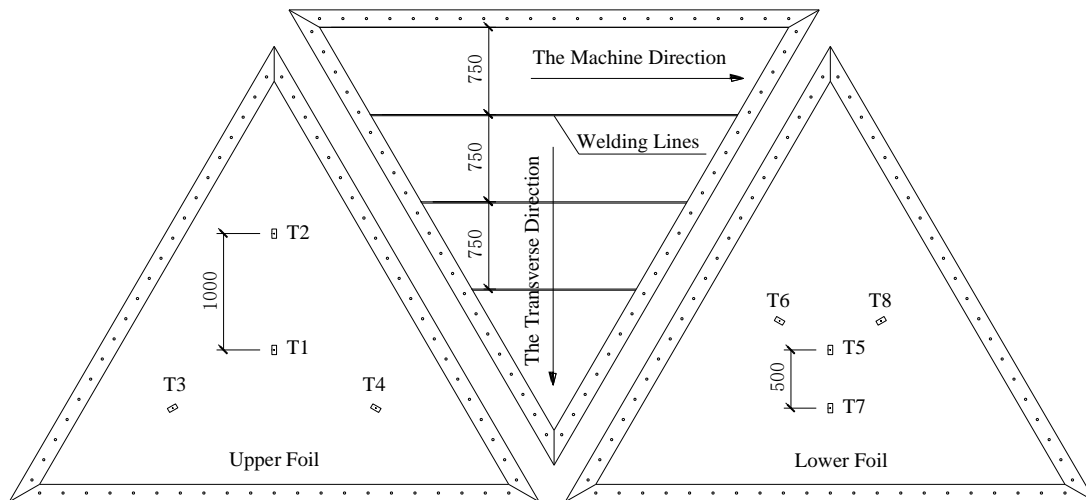


Fig. 6 Welding lines and creep displacement measuring points in cushion creep test

through the air inflation hole in 120 seconds, which enable similar loading time as those in S-2 uniaxial creep tests. When pressure reached 1845 Pa, loading test ceased and creep test began. To maintain a constant pressure at 1845 Pa in the bubble creep test, air pressure was monitored and controlled through air inflation. Displacements of the six measuring points were recorded by laser sensors. Time of creep test was 10 hours and temperature during tests was $20 \pm 2^\circ\text{C}$.

2.5 Cushion creep test

A full scale structural element test was performed to study the creep property of double-layer ETFE cushion. Cushion used in this test was in regular triangle shape, with each edge of 4000.0 mm.

The double-layer cushion was clamped by aluminum element, which was connected to steel beams by bolts. As illustrated in Fig. 5, a hole was set at the corner of the lower foil. It was for

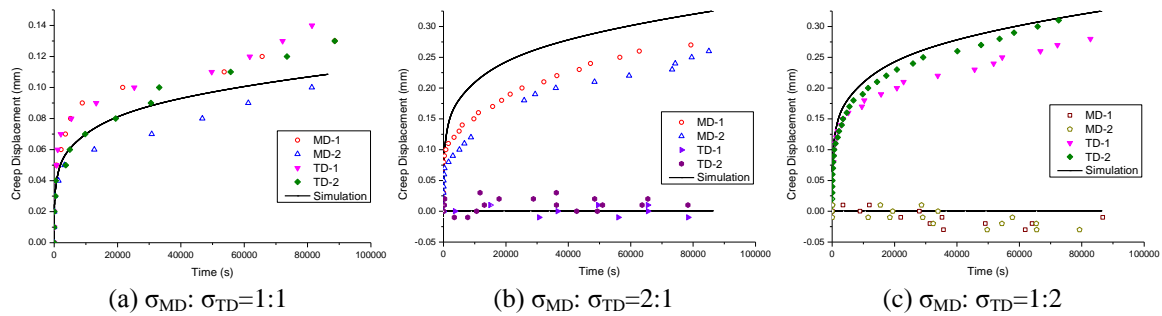


Fig. 7 Creep displacement in biaxial creep test

both air inflation and pressure sensor. The range of laser sensors was 40.00 mm and the accuracy was $\pm 0.15\%$. Additionally, the double-layer cushion was designed by shape finding analysis (Lee and Han 2011), in which inner pressure was 450 Pa. Under this inner pressure, stress in the cushion was identical at 3.56 MPa. The cushion was cut and welded to form its curve shape as form finding result. Welding lines and directions of foil were shown in Fig. 6. Also, as illustrated in Fig. 6, four displacement measuring points (T1-T4) were set in the upper foil and the other four points (T5 - T8) were set in the lower foil.

In the loading process, air was gassed through the hole at corner. To control the creep stress in cushion, inner air pressure was set as 825 Pa in this creep test. Considering the effect of strain rate, the time of loading in this test was set similar to those in S-2 uniaxial creep tests and was 120 seconds. After 120 seconds inflation process, creep test began and creep displacements of the upper and lower foils were recorded by eight laser sensors. The inner air pressure of cushion was kept constant through pressure control in creep test. Time of this creep test was 12 hours and temperature during tests was $20 \pm 2^\circ\text{C}$.

3. Results and discussion

3.1 Result of biaxial creep tests and conversion relation

Results of biaxial creep tests are shown in Fig. 7, in which specimens were biaxial tensioned under stresses: (1) $\sigma_{MD} = 6$ MPa, $\sigma_{TD} = 6$ MPa; (2) $\sigma_{MD} = 6$ MPa, $\sigma_{TD} = 3$ MPa; (3) $\sigma_{MD} = 3$ MPa, $\sigma_{TD} = 6$ MPa.

Along the direction that the stress is 6 MPa, the shape of creep curves is similar to that in uniaxial creep tests. But the creep displacements are almost zero along the other direction that the stress is 3 MPa. This is because of the shrinkage deformation causing by the creep deformation in the direction 6 MPa and Poisson's ratio effect. Meanwhile, Fig. 7 illustrates that creep displacements in the machine direction (MD) and the transverse direction (TD) are quite similar. Hence, creep coefficients in each direction are considered the same.

Uniaxial creep coefficients in identical stresses are adopted to simulate creep displacement in these biaxial creep tests. Yet, it is found creep displacements in the tests are much smaller than those simulation ones, meaning biaxial creep displacements are overestimated when simulated by merely uniaxial creep coefficients. On the other hand, while biaxial creep property is more valuable in engineering, uniaxial creep test is more convenient in laboratory. It is expected to

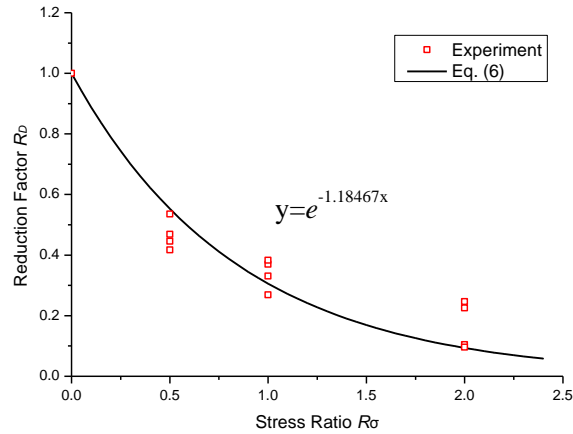


Fig. 8 Reduction factor R_D and stress ratio R_σ

estimate the biaxial creep displacement by uniaxial creep coefficients. Therefore, biaxial creep strain is suggested through a reduction factor R_D as following equation.

$$\begin{aligned} \varepsilon_{MD}(t) &= D_{MD} \sigma_{MD} \times R_D(R_{\sigma_{MD}}) - \nu D_{TD} \sigma_{TD} \times R_D(R_{\sigma_{TD}}) \\ \varepsilon_{TD}(t) &= D_{TD} \sigma_{TD} \times R_D(R_{\sigma_{TD}}) - \nu D_{MD} \sigma_{MD} \times R_D(R_{\sigma_{MD}}) \end{aligned} \tag{4}$$

in Eq. (4), the subscripts MD and TD represent the machine direction and the transverse direction, respectively. $\varepsilon_{MD}(t)$ and $\varepsilon_{TD}(t)$ are creep strains, σ_{MD} and σ_{TD} are stresses, D_{MD} and D_{TD} are transient uniaxial creep compliances with expression showing in Eq. (2), ν is Poisson’s ratio and equals to 0.42 (Galliot and Luchsinger 2011), $R_D(R_{\sigma_{MD}})$ and $R_D(R_{\sigma_{TD}})$ are biaxial reduction factors at the stress ratios $R_{\sigma_{MD}}$ and $R_{\sigma_{TD}}$, stress ratios is defined by Eq. (5).

$$R_{\sigma_{MD}} = \sigma_{TD} / \sigma_{MD} \text{ and } R_{\sigma_{TD}} = \sigma_{MD} / \sigma_{TD} \tag{5}$$

By means of Eq. (4), reduction factors in the biaxial creep tests are determined by the least squared method. As illustrated in Fig. 8, reduction factor R_D decreases with stress ratio R_σ . Obviously, R_D equals to 1.0 when R_σ is 0.0, in which foil is uniaxial tensioned. The reduction factor is then written as a function of stress ratio in exponential form, as shown in Eq. (6).

$$R_D(R_\sigma) = \exp(-1.18467 \times R_\sigma) \tag{6}$$

In biaxial tension condition, when the stress ratio is 1:1, reduction factor is about 0.3, meaning biaxial creep strain in this stress ratio is about one third as that simulated by uniaxial creep coefficients. And then, creep displacements in the biaxial creep tests of cruciform specimens are simulated by Eq. (4) and creep coefficients in Table 2, the results of which are plotted in Fig. 7.

As illustrated in Fig. 7, simulation curves embrace acceptable results comparing with test ones. While simulation curve locates among test data under stress ratio 1:1, curves are a bit higher in the direction that the stress is 6 MPa when stress ratio is 1:2 or 2:1, yet, this small deviation is also acceptable.

Meanwhile, this approach, determining biaxial creep displacements from uniaxial creep coefficients and a reduction factor, is quite convenient in application, because uniaxial creep tests are more practicable in laboratory and biaxial creep coefficients are suitable in creep analysis. This

approach combines advantages of both two.

3.2 Result of bubble creep test and simulation

On the basis of Schapery's nonlinear viscoelastic modelling in uniaxial form, Kennedy (1998), Chazal (2011), Wu (2014) developed finite element analysis of polymers for creep simulation. Finite Element Method (FEM) is also adopted in this section and programmed by FORTRAN in incremental formulation. Creep process of single-layer ETFE bubble test is simulated. Creep coefficients in numerical simulation are obtained from interpolation method and reduction factor, to take account of stress and biaxial effect respectively. To control strain increment between two successive times to approximate linear and do numerical simulation effectively, different time increments were set at different time ranges, namely time increment increased with time range. For example, to simulate creep behavior in 24 hours, time increment was set as 0.2 seconds in the initial 60 seconds and set as 40 seconds in the final 14 hours.

In this creep test, stress distributions in warp direction and weft direction are shown in Fig. 9, and distribution of stress ratios (between warp direction and weft direction) is plotted in Fig. 10. As illustrated in figures, at the center part of the bubble, stress in each direction is about 9.6 MPa and stress ratio is nearly 1.00. When it turns to the boundary part, for the constraints at the edge of

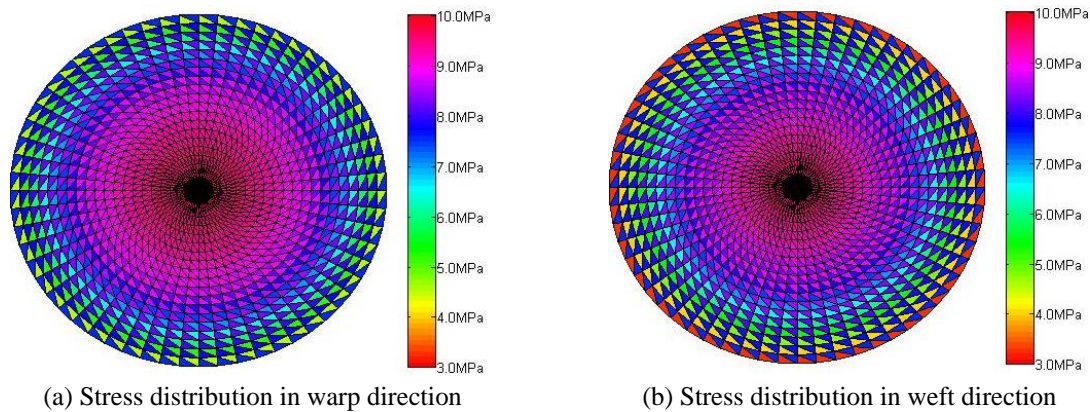


Fig. 9 Distribution of stresses in bubble creep test

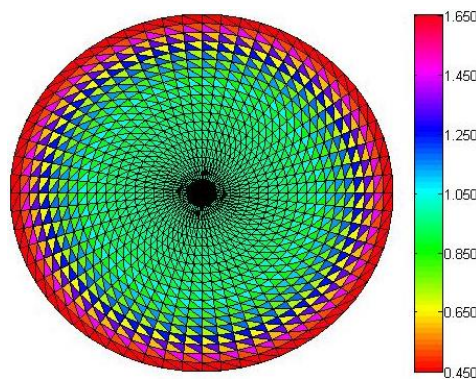


Fig. 10 Distribution of stress ratios in bubble creep test

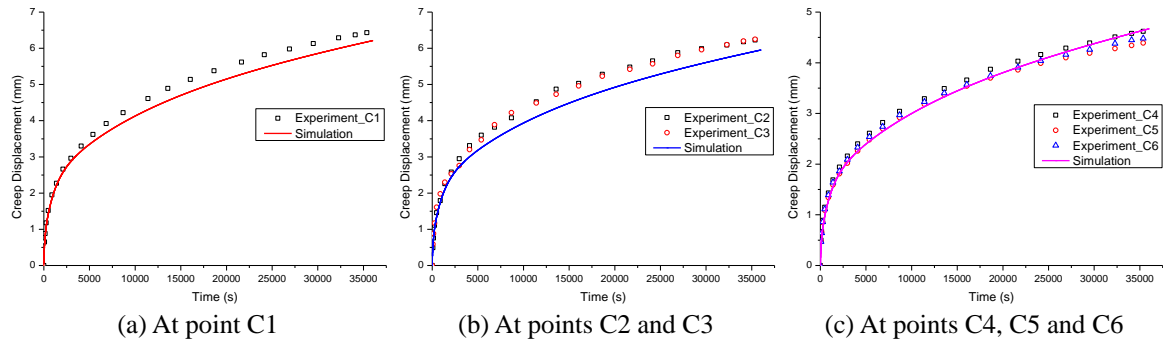


Fig. 11 Creep displacement in bubble creep test

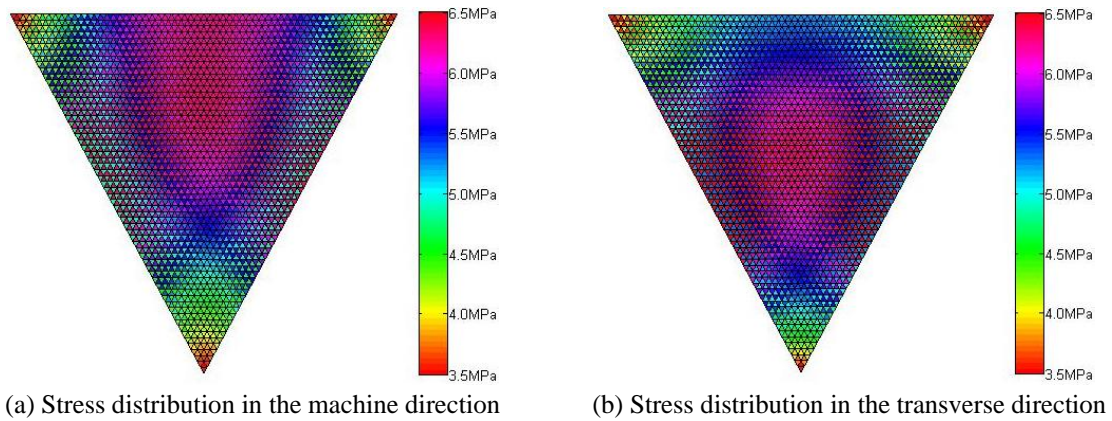


Fig. 12 Distribution of stresses in cushion creep test

circular specimen, minimum stresses in ETFE foil are 4.6 MPa in warp direction and 3.3 MPa in weft direction, and stress ratios range from 0.43 to 1.64.

Creep displacements of six measuring points, as those shown in Fig. 4 numbering from C1 to C6, are compared with numerical simulation results in Fig. 11. As illustrated, simulation results have a good agreement with test data. It means the interpolation method and biaxial reduction factors introduced in section 2.2 and 3.1 are practicable and valid to predict creep displacement of ETFE foil in biaxial tension condition.

3.3 Result of cushion creep test and simulation

Creep displacement of ETFE cushion creep test is also simulated by FEM. Because upper foil and lower foil in cushion were identical under inner pressure, and stress of ETFE foil was symmetry in two foils, merely upper foil is simulated in FEM.

By using FEM analysis, the maximum stress in the machine direction and the transverse direction is 6.4 MPa while the minimum stress is 3.5 MPa, when the inner pressure is 825 Pa. Detailed stress distribution in each direction is plotted in Fig. 12. Meanwhile, stress ratios (between the machine direction and the transverse direction) range from 0.75 to 1.37, as illustrated in Fig. 13.

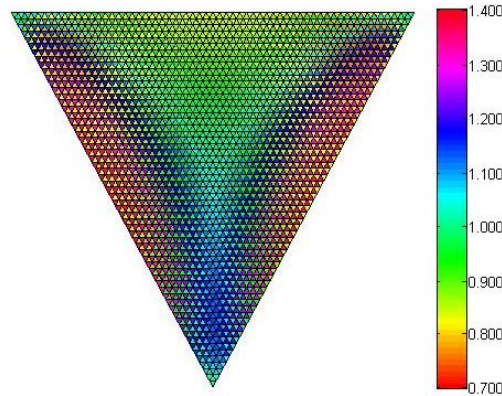


Fig. 13 Distribution of stress ratios in cushion creep test

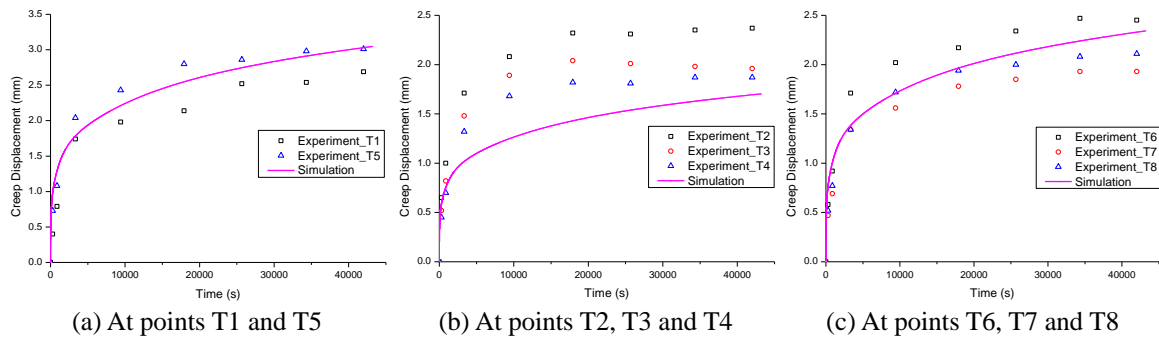


Fig. 14 Creep displacement in cushion creep test

As shown in Fig. 12 and Fig. 13, stresses and stress ratios in three sides are not the same. This is because of the direction of meshing. In the FEM model of this triangle cushion, the horizontal direction of mesh was set parallel to the machine direction of ETFE foil, and the vertical direction of mesh was set parallel to the transverse direction, as shown in Fig. 6. Meanwhile, one side of this triangle cushion was aligned with the horizontal direction while the other two were not. So, stresses and stress ratios in the cushion were under vertical axial symmetry. Yet, stress conditions and creep displacements in these three sides kept identical.

Creep displacements of eight measuring points (T1 to T8 as illustrated in Fig. 6) are compared with simulation ones in Fig. 14. Simulation results have a good agreement with test data at two center points (T1 and T5) and three displacement measuring points (T6 to T8) in the lower foil. It also verifies the validity of the interpolation method and biaxial reduction factors.

Yet, creep displacements in simulation are smaller than those in test at the corners of the upper foil (T2 to T4). It might come from two reasons. The first one is the fabrication and installation errors. It was difficult to get smooth surface at corner parts in the manufacture, especially for acute angles in such rectangle ETFE cushion. Meanwhile, the installment at corner parts was more sensitive to dimension errors. The other one is the wrinkles. For the acute angles, wrinkles occurred and were observed in which T2, T3 and T4 located. Affecting by these wrinkles, ETFE foil was more likely uniaxial tensioned rather than ideal biaxial tensioned, namely biaxial reduction factors might be overestimated in these parts.

4. Conclusions

This work presented a study about biaxial creep property of ETFE foil by means of three kinds of creep tests and numerical simulation. Results showed biaxial creep property was different with that in uniaxial one. To take account of this difference, biaxial creep strain was estimated by uniaxial creep coefficients and a reduction factor in this paper.

Biaxial creep tests of cruciform specimens were performed at three stress ratios. Results showed that creep displacements in biaxial tension tests counting about one third as those in uniaxial ones. A reduction factor was introduced to consider this biaxial effect on creep property. The reduction factor was suggested as the exponential function of stress ratio. Simulation results, obtained from uniaxial creep test data and reduction factors, showed a good agreement with the biaxial creep test data.

A single-layer ETFE bubble creep test and a double-layer ETFE cushion creep test were performed. The creep displacements of two tests were recorded. Numerical simulation of these two creep tests was carried out by FEM. Biaxial creep property of ETFE foil was considered in simulation. Results of test and simulation in circular bubble creep test verified the interpolation method and the reduction factor. In triangle ETFE cushion creep test, creep displacements at center points and lower foil were simulated well by FEM.

Biaxial creep property of ETFE foil and the reduction factors suggested in this paper are all investigated in room temperature and constant strain rate, while temperature and strain rate both have significant effects on time dependent behavior of this polymeric material. Further investigation would be necessary to develop the understanding of biaxial creep property of ETFE foil in different temperatures and strain rates.

Acknowledgements

This work is supported by National Natural Science Foundation of China (No. 51478333).

References

- Ambroziak, A. and Klosowski, P. (2014), "Mechanical properties for preliminary design of structures made from PVC coated fabric", *Constr. Build. Mater.*, **50**, 74-81.
- Charbonneau, L., Polak, M.A. and Penlidis, A. (2014), "Mechanical properties of ETFE foils: Testing and modelling", *Constr. Build. Mater.*, **60**, 63-72.
- Chazal, C. and Pitti, R.M. (2011), "Incremental constitutive formulation for time dependent materials: creep integral approach", *Mech. Time Depend. Mater.*, **15**(3), 239-253.
- Chung, K. and Ryou, H. (2009a), "Development of viscoelastic/rate-sensitive-plastic constitutive law for fiber-reinforced composites and its applications. Part I: Theory and material characterization", *Compos. Sci. Technol.*, **69**(2), 284-291.
- De Focatiis, D. and Gubler, L. (2013), "Uniaxial deformation and orientation of ethylene-tetrafluoroethylene films", *Polym. Test.*, **32**(8), 1423-1435.
- Galliot, C. and Luchsinger, R.H. (2011), "Uniaxial and biaxial mechanical properties of ETFE foils", *Polym. Test.*, **30**(4), 356-365.
- Hu, J.H., Chen, W.J., Zhao, B. and Song, H. (2014), "Experimental studies on summer performance and feasibility of a BIPV/T ethylene tetrafluoroethylene (ETFE) cushion structure system", *Energ. Build.*, **69**, 394-406.

- Hu, J.H., Chen, W.J., Luo, R.J., Zhao, B. and Sun, R. (2014), "Uniaxial cyclic tensile mechanical properties of ethylene tetrafluoroethylene (ETFE) foils", *Constr. Build. Mater.*, **63**, 311-319.
- Huang, X.K., Liu, G., Liu, Q. and Bennison, S.J. (2014), "An experimental study on the flexural performance of laminated glass", *Struct. Eng. Mech.*, **49**(2), 261-271.
- Kawabata, M. (2007), "Viscoplastic Properties of ETFE Film and Structural Behavior of Film Cushion", *Proceedings of the IASS Symposium*, Venice, Italy, December.
- Kawabata, M. and Moriyama, F. (2006), "Study on viscoelastic characteristics and structural response of film membrane structures", *Proceedings of the IASS Symposium*, Beijing, China, October.
- Kennedy, T.C. (1998), "Nonlinear viscoelastic analysis of composite plates and shells", *Compos. Struct.*, **41**(3), 265-272.
- Kennedy, T.C. and Wang, M. (1994), "Three-dimensional, nonlinear viscoelastic analysis of laminated composites", *J. Compos. Mater.*, **28**(10), 902-925.
- Kim, J. and Muliana, A. (2010), "Time-dependent and inelastic behaviors of fiber- and particle hybrid composites", *Struct. Eng. Mech.*, **34**(4), 525-539.
- Klosowski, P., Komar, W. and Woznica, K. (2009), "Finite element description of nonlinear viscoelastic behaviour of technical fabric", *Constr. Build. Mater.*, **23**(2), 1133-1140.
- LeCuyer, A. (2008), *ETFE Technology and Design*, Birkhauser, Basel, Switzerland.
- Lee, K.S. and Han, S.E. (2011), "Geodesic shape finding of membrane structure with geodesic string by the dynamic relaxation method", *Struct. Eng. Mech.*, **39**(1), 93-113.
- Li, Y.T. and Wu, M.E. (2015), "Uniaxial creep property and viscoelastic-plastic modelling of ethylene tetrafluoroethylene (ETFE) foil", *Mech. Time-Depend. Mat.*, DOI 10.1007/s11043-014-9248-2.
- Pandini, S. and Pegoretti, A. (2011), "Time and temperature effects on Poisson's ratio of poly(butylene terephthalate)", *Express Polym. Lett.*, **5**(8), 685-697.
- Papanicolaou, G.C., Zaoutos, S.P. and Cardon, A.H. (1999a), "Further development of a data reduction method for the nonlinear viscoelastic characterization of FRPs", *Compos. Part A: Appl. Sci. Manuf.*, **30**(7), 839-848.
- Papanicolaou, G.C., Zaoutos, S.P. and Cardon, A.H. (1999b), "Prediction of the non-linear viscoelastic response of unidirectional fiber composites", *Compos. Sci. Technol.*, **59**(9), 1311-1319.
- Robinson-Gayle, S., Kolokotroni, M., Cripps, A. and Tanno, S. (2001), "ETFE foil cushions in roofs and atria", *Constr. Build. Mater.*, **15**(7), 323-327.
- Ryou, H. and Chung, K. (2009b), "Development of viscoelastic/rate-sensitive-plastic constitutive law for fiber-reinforced composites and its applications Part II: Numerical formulation and verification", *Compos. Sci. Technol.*, **69**(2), 292-299.
- Schapery, R.A. (1969), "On the characterization of nonlinear viscoelastic materials", *Polym. Eng. Sci.*, **9**(4), 295-310.
- Williams, M.L., Landel, R.F. and Ferry, J.D. (1955), "The temperature dependence of relaxation mechanisms in amorphous polymers and other glass-forming liquids", *J. Am. Chem. Soc.*, **77**(14), 3701-3707.
- Wu, M.E. and Liu, J.M. (2008), "Experimental studies on ETFE cushion model", *Proceedings of the IASS Symposium*, Acapulco, Mexico, October.
- Wu, M.E. and Li, Y.T. (2014), "Revised finite element formulation for membrane creep analysis", *Proceedings of the IASS Symposium*, Brasilia, Brazil, September.
- Zhang, Y.Y., Zhang, Q.L., Li, Y. and Chen, L. (2014), "Research on the mechanical properties of membrane connections in tensioned membrane structures", *Struct. Eng. Mech.*, **49**(6), 745-762.